Impact of hydraulic model resolution and loss of life model modification on flood fatality risk estimation

Case study of the Bommelerwaard, The Netherlands

Brussee, Anneroos R.; Bricker, Jeremy D.; De Bruijn, Karin M.; Verhoeven, Govert F.; Winsemius, Hessel C.; Jonkman, Sebastiaan N.

DOI
10.1111/jfr3.12713

Publication date
2021

Document Version
Final published version

Published in
Journal of Flood Risk Management

Citation (APA)
Brussee, A. R., Bricker, J. D., De Bruijn, K. M., Verhoeven, G. F., Winsemius, H. C., & Jonkman, S. N. (2021). Impact of hydraulic model resolution and loss of life model modification on flood fatality risk estimation: Case study of the Bommelerwaard, The Netherlands. *Journal of Flood Risk Management*, *14*(3), 1-15. Article e12713. https://doi.org/10.1111/jfr3.12713

Received: 12 August 2020 | Revised: 10 February 2021 | Accepted: 19 February 2021

DOI: 10.1111/jfr3.12713

ORIGINAL ARTICLE

CIWEM Chartered Institution of Water and Environmental Management | Journal of Flood Risk Management | WILEY

Impact of hydraulic model resolution and loss of life model modification on flood fatality risk estimation: Case study of the Bommelerwaard, The Netherlands

Anneroos R. Brussee[1,2] | **Jeremy D. Bricker**[2,3] | **Karin M. De Bruijn**[1] | **Govert F. Verhoeven**[4] | **Hessel C. Winsemius**[4,5] | **Sebastiaan N. Jonkman**[2]

[1]Flood Risk Management, Deltares, Delft, South Holland, The Netherlands

[2]Department of Hydraulic Engineering, Delft University of Technology, Delft, South Holland, The Netherlands

[3]Civil and Environmental Engineering, University of Michigan, Ann Arbor, Michigan

[4]Catchment and Urban Hydrology, Deltares, Delft, South Holland, The Netherlands

[5]Department of Water Management, Delft University of Technology, Delft, South Holland, The Netherlands

Correspondence
Jeremy D. Bricker, Department of Hydraulic Engineering, Delft University of Technology, Delft, South Holland, The Netherlands.
Email: j.d.bricker@tudelft.nl

Funding information
TKI Delta Technology Project TU02; Deltares

Abstract

Flood simulations are important for flood (fatality) risk assessment. This article provides insight into the sensitivity of flood fatality risks to the model resolution of flood simulations and to several uncertain parameters in the loss of life model used. A case study is conducted for river flooding in a polder in the Netherlands (the Bommelerwaard) where the Dutch approach for loss of life estimation is applied. Flood models with resolutions of 100, 25, and 5 m are considered. Results show locally increased mortality rates in higher resolution simulations nearby structures including road embankments, dikes, and culverts. This causes a larger maximum individual risk value (annual probability of death for a person due to flooding) which has consequences for safety standards based on the individual risk criterion. Mortality rate in the breach zone is also affected by representations of buildings as solid objects versus as roughness elements. Furthermore, changes in the loss of life estimation approach via alternative ways of including people's behaviour, building characteristics, and age of the population, have a significant impact on flood fatality risk. Results from this study can be used to support future risk assessments and decision making with respect to safety standards.

KEYWORDS

D-Flow Flexible Mesh, flood risk assessment, hydrodynamic modelling, individual risk, loss of life, model resolution, mortality function

1 | INTRODUCTION

Flood risk maps are used for various purposes such as visualising risk assessments, developing flood risk management strategies including spatial planning, and prioritising required measures (De Bruijn & Klijn, 2009). In some countries, such maps are also used for insurance purposes (de Moel, van Alphen, & Aerts, 2009). These are developed based on hydrodynamic models that simulate the flood characteristics of potential flood events. Hydrodynamic models are widely used for this cause, but can be computationally intensive (Teng et al., 2017).

Since modern software is becoming more advanced, hydrodynamic modelling can be performed with a higher

level of detail (Bermúdez & Zischg, 2018; Beven, 2007; Teng et al., 2017), especially if flexible or unstructured mesh software are used making it possible to apply finer model resolutions only in areas of interest and while avoiding large computation times. Also, more detailed input data are becoming accessible, such as more detailed digital elevation models (DEM) and land cover maps, for example, from remote sensing and satellite-derived data (Bates, 2012; Mason, Horritt, Hunter, & Bates, 2007; Papaioannou, Loukas, Vasiliades, & Aronica, 2016; Savage, Pianosi, Bates, Freer, & Wagener, 2016; van der Sande, de Jong, & de Roo, 2003). Higher-resolution DEMs and land cover maps provide more accurate estimations of local topography and friction and can be of use to reduce uncertainty for inundation modelling.

There is increased attention towards the consequences of floods (De Moel et al., 2009; Kron, 2005) and much research has been done to identify the uncertainty of input data of hydrodynamic models on flood inundation mapping and resulting damages (Apel et al., 2009; Chen et al., 2016; Papaioannou et al., 2016; Pappenberger, Beven, Ratto, & Matgen, 2008; Parodi et al., 2020). The effect of the model resolution specifically has also been assessed in literature, for example, by Fewtrell, Bates, Horritt, and Hunter (2008), Asselman (2009), and Savage, Bates, Freer, Neal, and Aronica (2016). Especially, urban (two-dimensional) flood modelling is considered in the literature as a challenge due to the complexity of the area, blockage effects, the presence of obstacles and the interplay between buildings and surface flow (Hunter et al., 2008; Mignot, Paquier, & Haider, 2006). For example, Yu and Lane (2006) state that the inundation extent and timing of inundation for urban fluvial flooding are sensitive to the spatial resolution due to smoothing of the elevation model and blockage effects resulting in poorer representativeness of small-scale flows. Asselman (2009) explains as a guiding principle that a 100 m resolution is appropriate for relatively flat areas, while in villages the resolution should be on the order of 10 m or smaller to prevent blockage effects, depending on the size of the streets. It is frequently mentioned in the literature that model resolution in urban areas should be linked to the dimensions of the buildings (Asselman, 2009; Dottori, di Baldassarre, & Todini, 2013; Fewtrell et al., 2008; Schubert & Sanders, 2012) and assessing flood (building) damage in urban areas at small scales or even at the individual object level (micro-scale) has become a trend (Bermúdez & Zischg, 2018; Ernst et al., 2010; Shen, Qian, Chen, Chi, & Wang, 2019). The optimal model resolution must be based on a trade-off between accuracy and computational effort, the modelling objectives and complexity of the area.

The relation between flood simulation resolution and resulting flood fatality risk has not been investigated in the literature. There are studies about the modelling of loss of life and which factors to include (e.g., Aboelata & Bowles, 2008; di Mauro, de Bruijn, & Meloni, 2012; Jonkman, 2007; Lumbroso, Sakamoto, Johnstone, Tagg, & Lence, 2011; Priest, 2007), but the impact of hydraulic model resolution on the outcomes is not yet clear. Therefore, this article focuses on the relation between the hydraulic model resolution and the resulting mortality rates and flood risk estimates.

To investigate this relation, we conduct a case study in the Netherlands for which the Dutch loss of life estimation approach (Jonkman, 2007; Maaskant, Jonkman, & Kok, 2009) is applied. This approach is based on data from the last major Dutch flood event, in 1953, when large parts of the country were flooded unexpectedly due to multiple breaches in the coastal defences. This 1953 event is called the "Watersnoodramp" and caused 1,795 direct fatalities (Jonkman, 2007). Such large-scale flooding has not happened since in the Netherlands; hence, the Dutch mortality functions, providing mortality rate as a function of flood characteristics, are largely based on the 1953 data. However, many circumstances and factors which influence mortality rates have changed since 1953, such as socio-economic conditions and building quality. The potential effect of these changes on flood fatality risks is also analysed in this article.

The Dutch safety standards are based on the criteria individual risk, societal risk, and economic risk (Jonkman, Jongejan, & Maaskant, 2011; Slootjes & van der Most, 2016). Loss of life plays a key role in the first two criteria and also influences the third criterion in which fatalities are valued in monetary terms. The individual risk, the annual probability of someone present at the location during the whole year to die due to a flood, must be lower than 10^{-5} per year as stated in the Dutch Water Act and is the decisive criterion for the Bommelerwaard.

This article starts with a description of the case study area, and the methodology of hydrodynamic modelling and the loss of life modelling in Section 2. The resulting flood characteristics and mortality rate (probability of death for an exposed individual in a specific location) and loss of life (number of fatalities) outcomes are analysed for different model resolutions in Section 3. Additionally, the sensitivity of the outcomes to changes in the mortality functions is analysed. Section 4 presents the discussion and Section 5 draws conclusions.

2 | METHODOLOGY

2.1 | Case study area

The Bommelerwaard is a Dutch polder enclosed by three rivers with a surface area of approximately 11,000 ha and

a population of around 50,000 inhabitants which are protected by a dike ring. The area is relatively flat and slopes slightly downward towards the west. The location and characteristics of the area are shown in Figure 1. The Meidijk is located in the western end of the polder. This is an old embankment which cuts the total dike ring area into two parts and plays an important role in the flood pattern. The rivers surrounding the polder are the Waal in the north and the Meuse in the South. The Waal is the larger river of the two.

2.2 | Hydrodynamic model

The hydrodynamic model is developed utilising the software D-Flow Flexible Mesh of the Delft3D FM Suite, which allows the user to apply finer resolutions for areas of interest by linking structured and unstructured meshes. D-Flow Flexible Mesh (D-Flow FM) has been widely validated for flood wave simulation (e.g., Hoch et al., 2017). Model resolutions of 100, 25, and 5 m are applied here. The 5 m resolution model is evaluated only for a subset of the domain (Zaltbommel), because the computation time would be too long if the total dike ring area would be modelled with this high resolution. Zaltbommel is the largest municipality in the Bommelerwaard and is located next to the river Waal (see Figure 1). The 5 m simulation includes also the area between the highway and railway on the southern side of the city.

In the case study, the embankment along the Waal river is assumed to breach in the northeast of the polder (see Figure 1). This location is based on the breach scenario of "Veiligheid Nederland in Kaart 2" (VNK2) for the standard flood wave ("maatgolf" in Dutch) at Hurwenen (Vergrouwe & Bossenbroek, 2010; Projectbureau VNK2, 2011). This location is the worst-case scenario for this area and a breach there would contribute most to the overall individual risk. The breach is modelled using an inflow over a horizontal boundary with a width of 210 m. The inflow, or breach discharge, is assumed to increase from zero to the maximum of 2,754 m^3/s in 1 day and then decreases linearly to zero again in 7 days. The flood simulations are executed for 12 days, as maximum flood conditions are reached within this flood simulation time.

The DEM originates from AHN3, 2019 ("Actueel Hoogtebestand Nederland 3 (Database for elevations in the Netherlands 3),") with a 5 m resolution which was aggregated from 0.5 m data, and excludes vegetation and

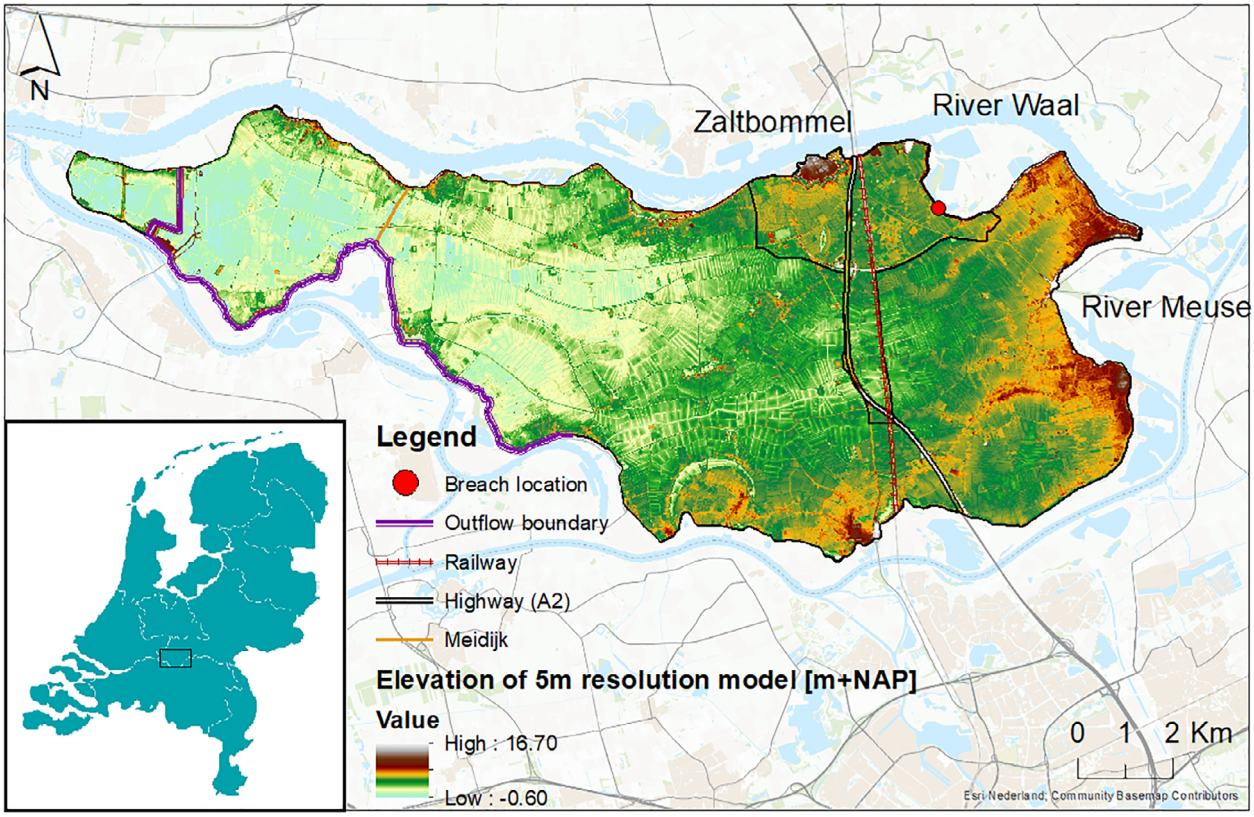

FIGURE 1 Overview of the Bommelerwaard area in the Netherlands. Elevations are relative to the Normaal Amsterdams Peil (NAP) vertical datum, which roughly indicates mean sea level on the Dutch coast

buildings. The 100 and 25 m elevation models are aggregated from the 5 m model using median grid cell values. Median values are taken to limit the impact of outliers. The elevations of embankments and raised roads, which are crucial for the flood pattern, are based on the maximum values in each grid cell, and are corrected at underpasses. In this study, the obstacles are assumed to withstand water levels until their maximum elevation, after which overtopping occurs.

The roughness grid is based on the land use classes of LGN6, 2008 ("Landelijk Grondgebruik Nederland 6 (Database for land use in the Netherlands),"). These land use classes are available with 25 m resolution and are translated into White–Colebrook roughness coefficients based on the conversion table of de Bruijn and Slager (2018), as shown in Brussee (2020). They are aggregated to 100 m resolution by grid cell mean values. For the 5 m model, the urban area is modelled with two different approaches for building representation:

1. The urban areas (including buildings) have a higher hydraulic roughness than their rural surroundings, or
2. The buildings are schematized as solid objects with a higher elevation than the floodwaters.

The first approach assumes that the buildings and their surroundings (streets, gardens, parked cars, etc.) have a roughness equal to a White–Colebrook value of 10 m, while the surrounding rural areas have a roughness of 1 m. In the second approach, buildings are represented as 10 m high blocks located at the footprints of the buildings, which are based on data of the geodatabase of BAG, 2017 ("Basisregistratie Adressen en Gebouwen (Database for building characteristics),"), thereby forcing floodwater to flow around the buildings.

To allow flood water to flow over the embankment out of the area at the downstream site of the polder, fixed weirs with spatially varying elevation equal to local embankment elevation are added to the model. The location of the southern outflow boundary is indicated in purple in Figure 1. For further details on the hydrodynamic model, set-up reference is made to Brussee (2020).

2.3 | Loss of life model

In the Dutch loss of life estimation approach, the number of fatalities is estimated by multiplying the mortality rate by the number of people exposed to flooding in the area at risk:

$$N = N_{PAR} * F_D * (1 - F_E)$$

where N is the number of fatalities [persons], N_{PAR} is the number of people at risk [persons], F_D is the mortality rate [−], and F_E is the evacuation fraction [−]. Figure 2 shows an overview, it includes the variables from the above equation and shows that the number of people at risk (N_{PAR}) is also reduced in case of shelter.

Mortality rate is the ratio between the number of fatalities and the number of people exposed and can be estimated by the mortality functions of Jonkman (2007) and Maaskant et al. (2009). These functions relate the flood characteristics water depth, flow velocity, and water level rise rate to mortality rates. All other factors which influence mortality rates, such as the exposure characteristics and social vulnerability, are included implicitly in the data. The functions of Maaskant et al. (2009) distinguish four flood zones as shown in Table 1: a breach zone with high mortality rate, a zone with rapidly rising water, a zone with more moderate conditions (remaining zone) and a transition zone. Table 1 shows the definition of the zones and Figure 3 shows the mortality functions as a function of the flood depth.

The Dutch standard Damage & Mortality Module (SSM2017) (Slager & Wagenaar, 2017) is used to calculate mortality based on the functions above. D-Flow FM generates NetCDF files (NC format) that store the multi-dimensional flow data output. The grids for the flood characteristics are converted from NC format to TIF format by Python scripts, and are then imported into SSM2017. SSM2017 generates the flood fatalities, people affected, and the mortality rates.

The individual risk, the probability per year of a person dying in a flood, is calculated for each neighbourhood defined by Statistics Netherlands (CBS) in 2008. The Bommelerwaard has 45 neighbourhoods with an average size of 340 ha; an overview of neighbourhoods is tabulated in Brussee (2020).

This study considers one flood scenario for simplification and therefore, estimates the individual risk per neighbourhood by multiplying the probability of flooding by 1 minus the evacuation fraction, times the mortality rate:

$$\mathrm{IR}(n) = P_f * (1 - F_E) * F_{D,\mathrm{median}}(n)$$

where $\mathrm{IR}(n)$ is the individual risk in neighbourhood n [per year], P_f is the probability of flooding [per year], F_E is the evacuation fraction [−], $F_{D,\mathrm{median}}(n)$ is the median mortality rate of the neighbourhood n [−]. The median mortality rate is used to reduce the influence of outliers, for example, if accidently a waterway or ditch is not excluded from the analysis. For dike trajectory 38-1 (the northern Bommelerwaard), the embankments are designed to withstand a flood with a probability of

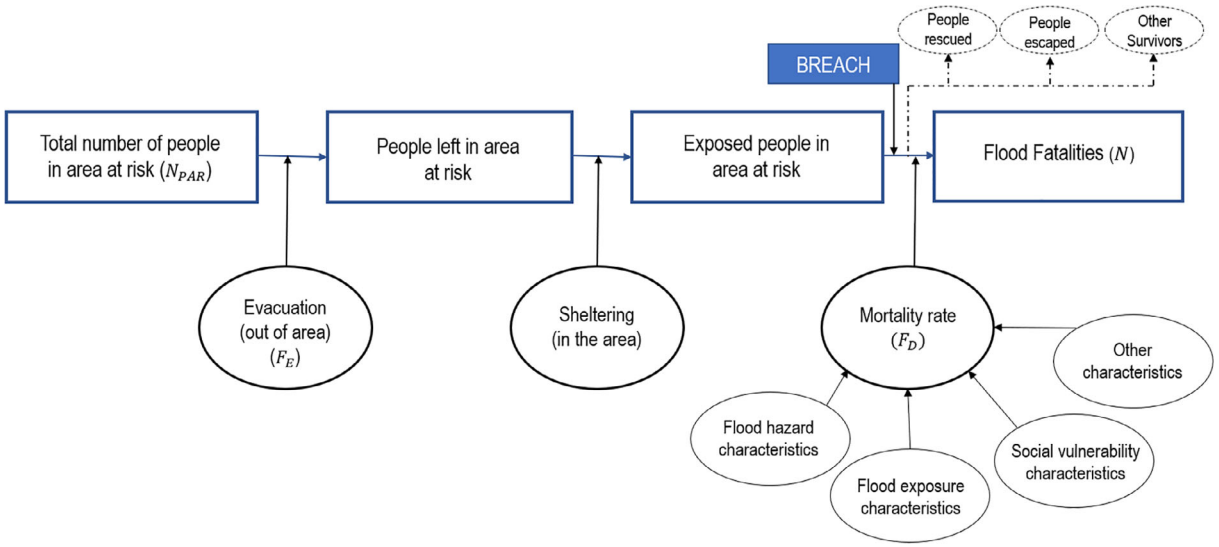

FIGURE 2 Overview of Dutch loss of life estimation approach, based on Jonkman (2007) and Di Mauro et al. (2012)

TABLE 1 Mortality functions of Jonkman (2007), adapted by Maaskant et al. (2009)

Zone	Definition of zone	Mortality function
Breach zone	If $h*v \geq 7$ m^2/s and $v \geq 2$ m/s	$F_{D,B} = 1$
Rapidly rising water zone	if ($h \geq 2.1$ m and $w \geq 4$ m/hr) and ($h*v < 7$ m^2/s or $v < 2$ m/s)	$F_{D,S}(h) = \Phi_N\left(\frac{\ln(h)-\mu_N}{\sigma_N}\right)$ with $\mu_N = 1.46$ and $\sigma_N = 0.28$
Transition zone	if ($h \geq 2.1$ m and $0.5 \leq w < 4$ m/hr) and ($h*v < 7$ m^2/s or $v < 2$ m/s)	$F_D(h) = F_{D,O} + (w-0.5) * \left(\frac{F_{D,S}-F_{D,O}}{3.5}\right)$
Remaining zone	if (w < 0.5 m/hr or ($h < 2.1$ m and $w \geq 0.5$ m/hr)) and ($h*v < 7$ m^2/s or $v < 2$ m/s)	$F_{D,O}(h) = \Phi_N\left(\frac{\ln(h)-\mu_N}{\sigma_N}\right)$ with $\mu_N = 7.60$ and $\sigma_N = 2.75$

Note: F_D = Mortality rate [−]; $F_{D,B}$ = Mortality rate in the breach zone [−]; $F_{D,S}$ = Mortality rate in the rapidly rising water zone [−]; $F_{D,O}$ = Mortality rate in the remaining zone [−]; h = Water depth [m]; v = Flow velocity [m/s]; w = Water level rise rate (averaged over the first 1.5 m water depth, counted from 2 cm) [m/hr]; Φ_N = Lognormal distribution; μ_N = Mean value from ln(h); σ_N = *SD* of ln(h).

exceedance of 1/1,250 per year and therefore, we assume here the flood probability to be 1/1,250 per year. The evacuation fraction applied in the Deltaprogramme to assess safety standards is 0.56 (Slootjes & Wagenaar, 2016). The mortality rate maps are corrected by excluding waterways and cells which are not flooded because the inclusion of waterways can results in an overestimation, and dry cells in an underestimation, of the individual risk.

The sensitivity of the mortality rate to the water arrival time, building quality, and age of the population is analysed by the following modifications to the mortality functions:

- *Inclusion of the water arrival time by escape fractions*: In areas where it takes long for the water to arrive, people may escape from the area, reducing the number of people present in the endangered area:

$$N = N_{\mathrm{PAR}} * F_D * (1-F_E) * (1-F_{\mathrm{esc}})$$

where F_{esc} is the escape fraction. The escape fraction, introduced by De Bruijn and Slager (2014), is thus in addition to the evacuation fraction. An example of escape fractions for the Bommelerwaard is shown in Table 2.

- *Inclusion of improved building characteristics*: For the rapidly rising water zone, a first approximation is available in which the mortality rate is assumed to be lower ($\mu_N = 1.68$ and $\sigma_N = 0.37$) due to the improved quality of the buildings nowadays compared to 1953,

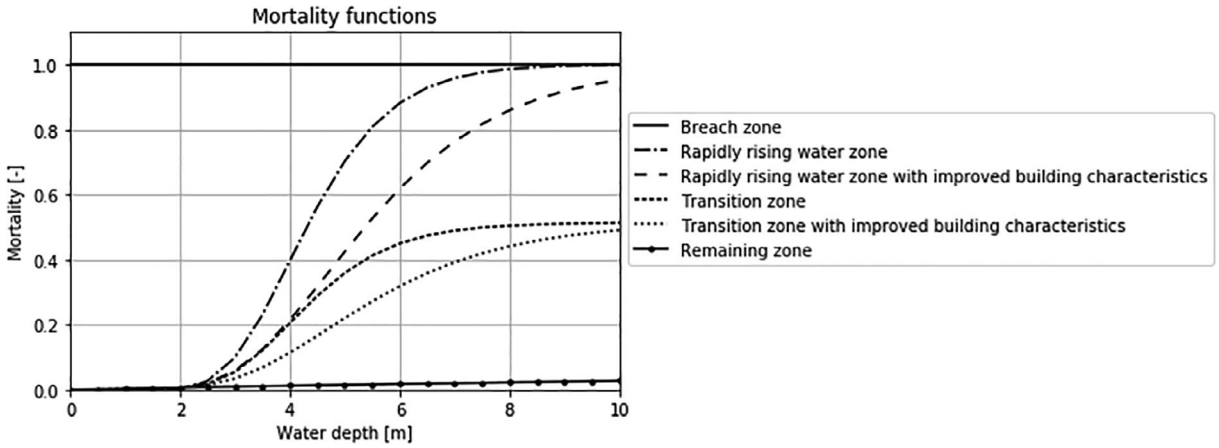

FIGURE 3 Overview of the Dutch mortality functions, including the functions for the improved building characteristics (assumed building distribution of 50–50 for brick cavity walls and concrete). The mortality functions for the transition zone in this figure are based on a water level rise rate of 2.25 m/hr

TABLE 2 Example of escape fractions by the inclusion of water arrival time for the Bommelerwaard, based on De Bruijn and Slager (2014)

Water arrival time (hr)	Escape fraction (%)	(1 - escape fraction) (%)	Example of people present after evacuation and escape ($F_E = 0.56$) (%)
0–4	0	100	44
4–8	15	85	37
8–12	30	70	31
12–16	45	55	24
16–20	60	40	18
20–24	75	25	11
>24	90	10	4

from which base-case fragility functions were formulated (Asselman, 2005; Jansen et al., 2020; Jonkman, 2007). This corresponds with an assumed building distribution of 50–50 for brick cavity walls and concrete. The transition zone is adapted similarly (see Figure 3).

- *Inclusion of people's vulnerability by correcting for age*: Elderly residents are assumed to be more vulnerable to large-scale flooding (Brussee, 2020; Jonkman et al., 2009). More elderly are present in society nowadays due to "ageing" compared to 1953: CBS data show that 10% of the population was aged over 65 in 1953 while in 2019 this was 19%. This observation can be used to correct the mortality rate for the ageing effect. The inclusion of age is explored in two ways: (a) correcting the overall mortality rate and (b) correcting the mortality rate per neighbourhood. The details on the inclusion of age are given in Appendix.

The sensitivity analyses are conducted with the 100 m resolution model as the base case.

3 | RESULTS

The results of the sensitivity analysis for model resolution are explained in Section 3.1 and the results for the sensitivity analysis of the mortality determining factors are described in Section 3.2.

3.1 | Sensitivity to flood model resolution

3.1.1 | Resulting flood characteristics

The large-scale flood pattern resulting from all three model resolutions is similar. However, the 25 and 5 m

models lead to crucial differences in flood characteristics near small waterways, ditches, obstacles and structures. If obstacles and structures are modelled by including them in the flood model elevation data (which is common practice in two-dimensional flood simulation, as opposed to parameterizing them via the weir or orifice equations as is common in one-dimensional flood simulation), model resolution has a strong effect on flood depths, patterns, and rise rates nearby these obstacles.

First, consider the water depths. The Bommelerwaard is a low-lying area with large potential flood water depths. At some locations, for example, in Zaltbommel, the water depths in the 100 m model differ from the outputs produced with other model resolutions: depths are between 4 and 5 m in the 100 m resolution model, while in the 25 and 5 m models these are around 3–4 m (Figure 4). The water depth is an important parameter in the loss of life model and the slightly larger water depths in the 100 m model at locations with many inhabitants can result in more conservative loss of life estimates.

Differences in the flood pattern (Figure 5) are visible around obstacles. The floodwater is flowing from the breach location towards the west through the city of Zaltbommel. The highway and railway block the water flow, but an underpass allows the water to flow through. Since the underpass is modelled as a grid cell with a lower elevation than surrounding land, more discharge flows through the underpass in the 100 m model than in the 25 and 5 m models, resulting in shorter arrival times for the 100 m model in Zaltbommel (see Figure 5). Also, other locations show small differences near obstacles. Overtopping of obstacles occurs earlier in time in the 25 and 5 m models than in the 100 m model (such as the parcel southwest of the railway-highway intersection in the lower part of Figure 5). This results in shorter arrival times behind the obstacle in the 25 and 5 m models. Within the 100 m model, variations in obstacle crest elevation will be missed, since the maximum over a 100 m width is taken. In the 25 m model lower parts of obstacle crest elevations may be resolved.

The water level rise rate (averaged over the first 1.5 m water depth, counted from 2 cm) is shown to be locally different in each model. Overall, the rise rates are relatively low (<0.5 m/hr), but near obstacles, they can become very high (>0.5 m/hr) as obstacles can retain water. For example, the area between the highway and railway (indicated as area C on Figure 6 locater map) experiences high water level rise rates; Figure 6 shows that the rise rates here are higher over a larger area for the finer model resolutions compared to the 100 m model. Also, waterways (thin line features visible within areas A and B, and also to the southwest of area C, of Figure 6) stand out with high rise rates in the 25 and 5 m models, but people do not live in waterways and they are, therefore, not relevant.

3.1.2 | Differences between the building representations

The differences between the two building representations for the 5 m resolution model are primarily visible in the maximum flow velocity map, shown in Figure 7. In the area close to the breach, the flow velocities are very large, on the order of 4 m/s. The buildings close to the breach influence the flood pattern in building representation 2 since the water needs to flow around these buildings. This results in high velocities over a larger extent compared to building representation 1, which uses higher hydraulic roughness for the urban area including buildings. The differences in velocities are only visible in the area close to the breach until the railway. In the rest of the flooded area, the velocities are significantly lower and the impact of the building representation is small.

3.1.3 | Breach zone

In the Dutch loss of life approach, velocity is of relevance in the breach zone (Table 1), defined as the area with a

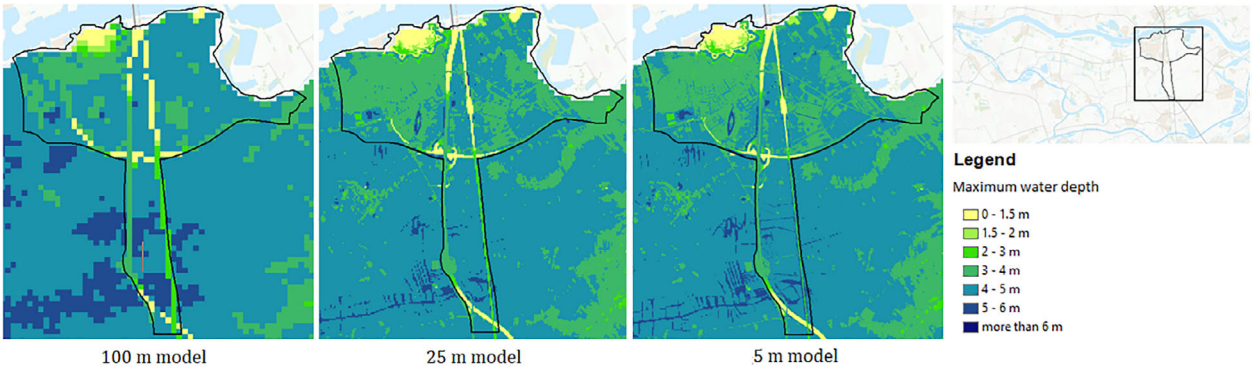

FIGURE 4 Results for the maximum water depth for the Zaltbommel area, which is indicated by the black outline

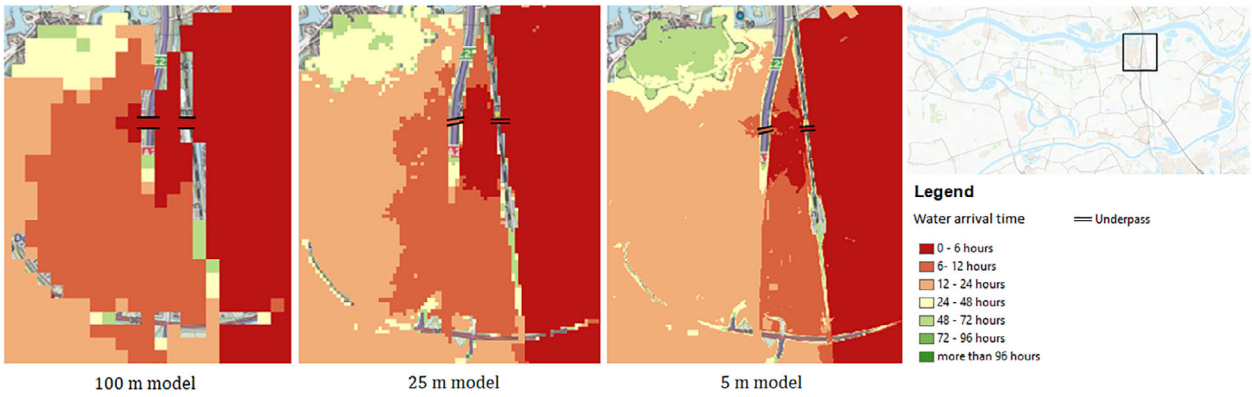

FIGURE 5 Results for the water arrival time zoomed in on the city centre of Zaltbommel

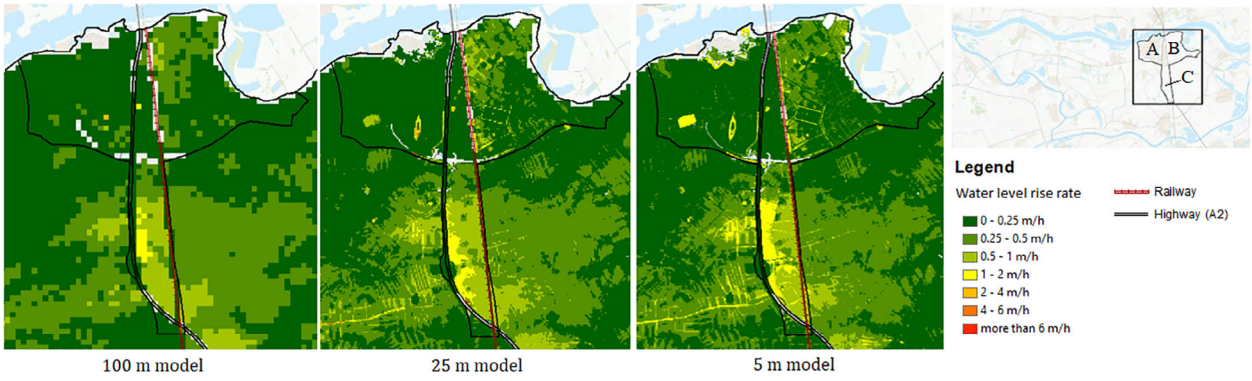

FIGURE 6 Results for the water level rise rate for the Zaltbommel area (averaged over the first 1.5 m water depth, counted from 2 cm)

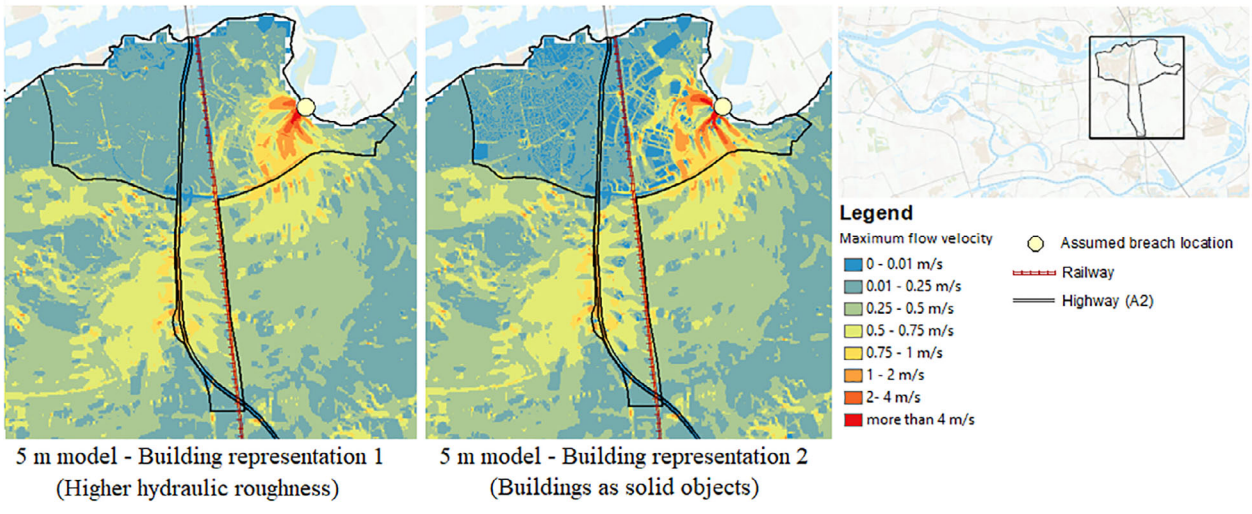

FIGURE 7 Results for the maximum flow velocity for the Zaltbommel area

velocity larger than 2 m/s and a depth-velocity product larger than 7 m^2/s. In the breach zone, the mortality rate is assumed to be 100% because of the severity of the flood characteristics in this zone.

Figure 8 shows an overview of the size of the breach zone for the different model resolutions and the two building representations for the 5 m model. This figure indicates that the breach zone has a larger area when a

finer model resolution is applied. The size of the breach zone area (defined according to the criteria in Table 1) is 60,000; 75,000; and 78,875 m^2, respectively, for the 100, 25, and 5 m (building representation 1) models, and 107,450 m^2 for the second building representation. This could be explained by the 100 m model averaging the peak velocities over a much coarser grid cell than the 25 and 5 m models, resulting in a lower magnitude than the finer models. Building representation 2 resulted in a significantly larger breach zone than building representation 1 due to funnelling of the water by the buildings, causing greater velocities over a larger spatial extent as a consequence.

3.1.4 | Mortality rate and loss of life assessment

The mortality rate maps for the 100 and 25 m models are shown in Figures 9 and 10 and provide the maximum mortality rates over the grid cells. The mortality rates are relatively high, between 1.1 and 1.5% (the green areas on the map). Overall, the 100 m model gives higher overall mortality rates due to slightly larger water depths in this model. Some locations experience increased mortality rates because of the combination of a large water depth and high water level rise rate, especially in front of and between obstacles. The finer model resolutions were

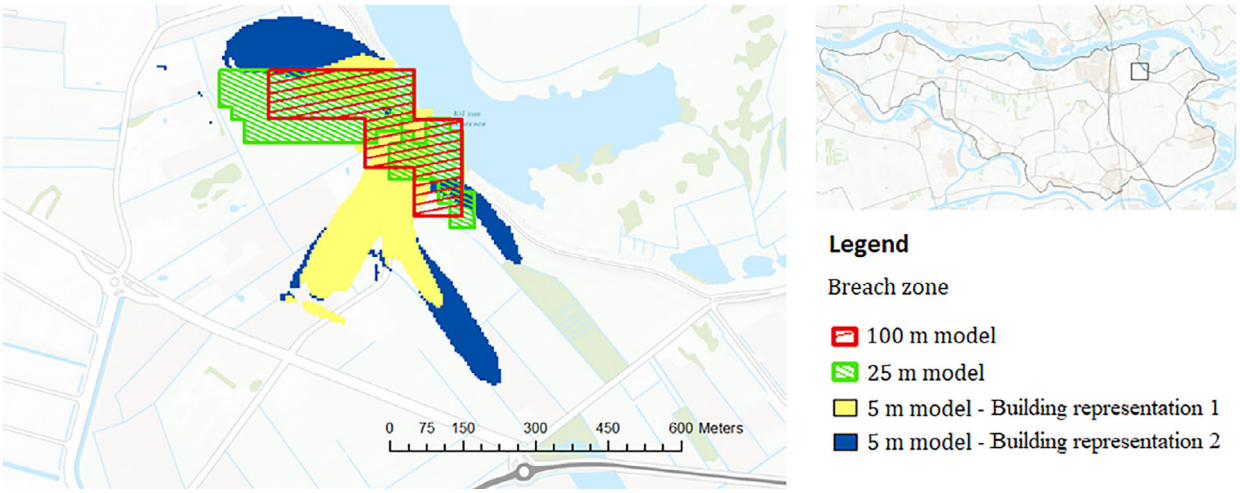

FIGURE 8 Extent of the breach zone per model resolution (and building representation)

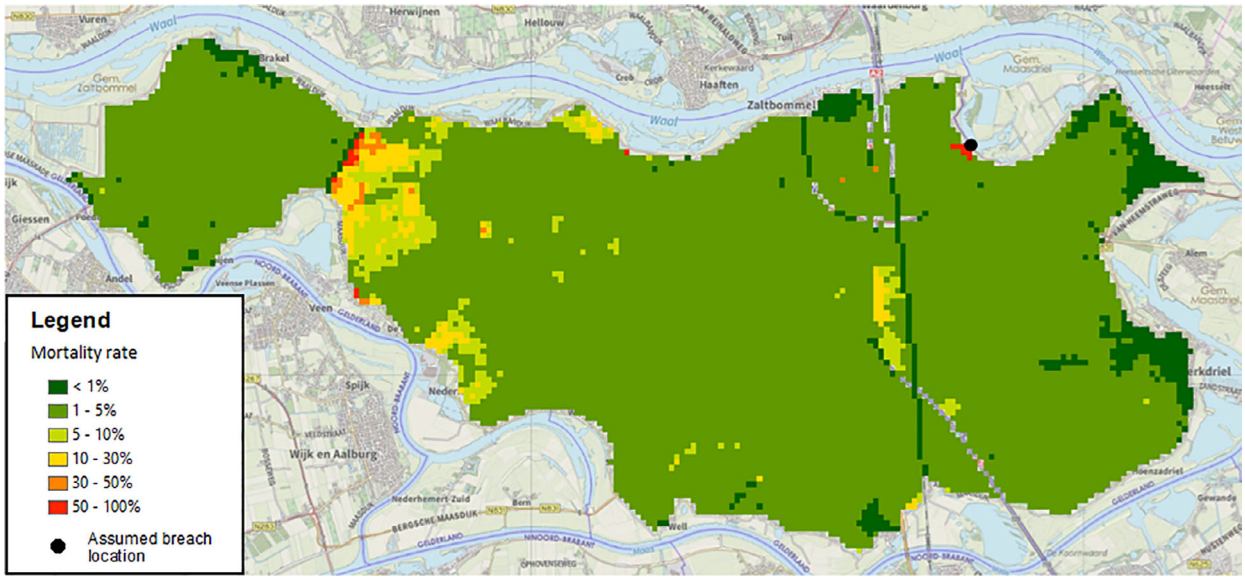

FIGURE 9 Mortality rate map for the 100 m model for the Bommelerwaard

found to have larger rise rates around obstacles and thus have larger localised mortality rates in specific areas. Also, local differences exist, such as the waterways being visible in the 25 m model and not in the 100 m model.

The mortality rate map is independent of the location of the inhabitants; hence, the maps show the dangerous locations regardless of the exposure. The mortality rate map is combined with the number of inhabitants to estimate the number of fatalities. This gives 598 fatalities for the 100 m model and 531 fatalities for the 25 m model.

Figure 11 shows the mortality rate maps for the area close to the breach. Overall, the mortality rate is the highest again in the 100 m model due to the larger water depths, but locally the finer model resolutions contain some dangerous spots, such as ditches. The area between the highway and railway stands out due to the higher mortality rate in the 25 and 5 m model due to the higher local water level rise rates. However, not many inhabitants are located in this area and thus the number of fatalities there is very small. Table 3 summarises the results and shows that the 100 m model results in the most fatalities and the highest mortality rate.

Table 3 also summarises the outcomes of the individual risk assessment. Corresponding to the higher overall mortality rate, the overall outcomes for the individual risk values per neighbourhood are higher for the 100 m model. However, the maximum individual risk value is critical for the safety standards and this value is higher for the 25 and 5 m models. The resulting median mortality rate in the most dangerous neighbourhood is thus higher for the finer model resolutions and this can be ascribed to the higher water level rise rates.

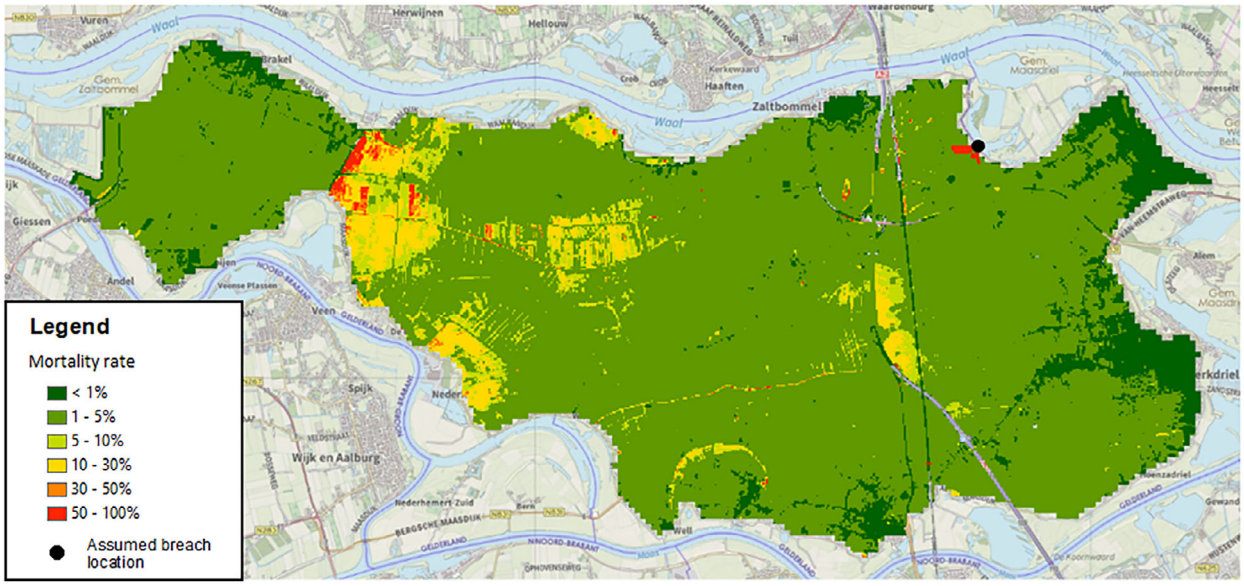

FIGURE 10 Mortality rate map for the 25 m model for the Bommelerwaard

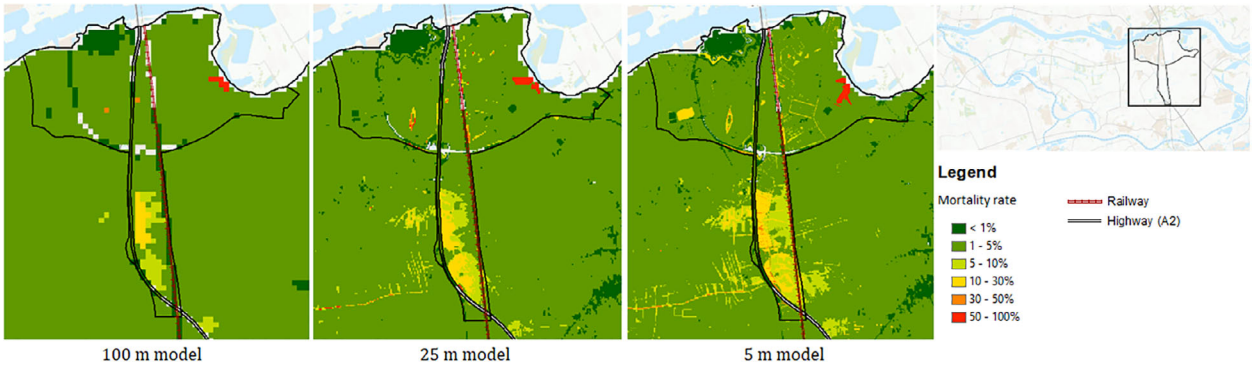

FIGURE 11 Mortality rate maps for the Zaltbommel area (the 5 m model result shown here uses building representation 1)

3.2 | Sensitivity to loss of life model

Table 4 summarises the results of the sensitivity analysis of the input of the Dutch loss of life estimation approach. The results vary per case and are discussed below.

3.2.1 | Inclusion of the water arrival time in escape fractions

Some parts of the Bommelerwaard have relatively long flood water arrival times (>12 hr). The inclusion of the water arrival time in the fatality risk assessment by introducing an escape fraction has a large impact on both the estimation of the fatalities and the individual risk. The number of estimated fatalities is reduced by more than 50%. All the neighbourhoods which were not in compliance with the maximum individual risk of 10^{-5} criterion in the base case, are after inclusion of escape fraction, in compliance with the individual risk criterion of $<10^{-5}$ per year. Moreover, the maximum individual risk is reduced by 60%.

3.2.2 | Inclusion of improved building characteristics

The inclusion of improved building characteristics in the rapidly rising water zone, and hence in the transition zone, has a limited impact (5%) on the number of fatalities. The impact on the individual risk is more significant, namely a reduction of the maximum value of 18%. The difference in impact on these two aspects relates to the base case, the 100 m model. The number of fatalities in the rapidly rising water and the transition zones specifically, is small and, therefore, the impact of this

TABLE 3 Results of the sensitivity analysis of the model resolutions. The Bommelerwaard has 45 neighbourhoods and the Zaltbommel area has 11 neighbourhoods. The maximum individual risk is the highest value of all individual risk values per neighbourhood

	Mortality rate and loss of life assessment			Individual risk assessment	
Case	Number of estimated fatalities	Inhabitants	Overall mortality rate (%)	Maximum individual risk (per year)	Number of neighbourhoods exceeding individual risk of 10^{-5} per year
Bommelerwaard					
100 m model	598	48,110	1.24	1.36×10^{-5}	3
25 m model	531	48,866	1.09	2.49×10^{-5}	2
Zaltbommel area					
100 m model	151	12,709	1.19	1.18×10^{-5}	1
25 m model	137	12,702	1.08	2.29×10^{-5}	1
5 m model (building representation 1)	140	12,702	1.10	2.73×10^{-5}	1

TABLE 4 Results of the sensitivity analysis of the input of the Dutch loss of life estimation approach using the 100 m model. The Bommelerwaard has 45 neighbourhoods. The maximum individual risk is the highest value of all individual risk values per neighbourhood

	Mortality rate and loss of life assessment			Individual risk assessment	
Factor included	Number of estimated fatalities	Inhabitants	Overall mortality rate (%)	Maximum individual risk (per year)	Number of neighbourhoods exceeding individual risk of 10^{-5} per year
Base case	598	48,110	1.24	1.36×10^{-5}	3
Escape fractions	208	48,110	0.43	5.40×10^{-6}	0
Improved building characteristics	571	48,110	1.19	1.12×10^{-5}	1
Ageing: Overall mortality rate	707	48,110	1.47	n/a	n/a
Ageing: Per neighbourhood	727	48,110	1.51	1.37×10^{-5}	3

modification on the total number of fatalities is limited. The individual risk does not depend on the number of inhabitants, but only on the mortality rate.

3.2.3 | Inclusion of people's vulnerability by age

The inclusion of age, either by correcting the overall mortality rate or per neighbourhood increase the number of fatalities by approximately 20%. The individual risk is influenced less by this factor for ageing: The number of neighbourhoods that do not comply with the individual risk criterion is the same as for the base case and also the maximum individual risk value is not influenced significantly. This limited impact is related to the spatial distribution of the elderly: the three most dangerous neighbourhoods have fractions of people aged over 65 just above or below 10%. The (median) mortality rate of a dangerous neighbourhood can increase significantly if it has a higher concentration of elderly than found in this case study.

4 | DISCUSSION

This article investigates the relationship between the hydraulic model resolution and resulting mortality rate and flood risk estimates. It aims to provide insight into the sensitivity of the spatial resolution of flood simulations in order to better assess flood fatality risk. Differences between the models have been found that impact the flood fatality risk for the case study of the Bommelerwaard in the Netherlands. The sensitivity of the mortality rates and fatality numbers to important factors which have changed since 1953 has also been evaluated.

In total, this study contributes to the better understanding of selecting the model resolution of the hydrodynamic model and the combination of flood simulations with loss of life models. The results of this study can be used to inform flood modellers, spatial planners, and emergency managers and to support decision-makers for flood risk management strategies.

The hydrodynamic model used in this study can be further optimised, for example, by connecting the river model to the flood model, improving the accuracy of the outflow boundaries, or including more aspects, such as drainage canals, rainfall and noise barriers. The sensitivity of the results on modelling assumptions such as the ability of an obstacle to retain water until its maximum elevation may have influenced the results and should be considered with care in future studies. Important to note is that the results obtained for the Bommelerwaard apply to a flat, low-lying area where structures strongly influence flow that otherwise tends to run overland and pond at the lowest elevation. Over steep, mountainous terrain, different behaviour is expected, because the topography of the river course is as important as the structures themselves (Bricker et al., 2017).

5 | CONCLUSIONS AND RECOMMENDATIONS

This section presents the conclusions we can draw from this study and gives recommendations for future research on hydrodynamic and loss of life modelling, and for flood risk managers overall.

5.1 | Sensitivity to flood model resolution

This study shows that, over a large spatial scale, the flood models of 100, 25, and 5 m resolution provide the same flood pattern and similar flood characteristics which can be used for mortality rate estimates, but that important differences are found at a smaller spatial scale near obstacles such as structures and underpasses, and near waterways. More discharge flows through the underpass in the 100 m model compared to the 25 and 5 m models when the underpass is modelled by elevation. Note that parameterizing structures as thin weirs or orifices (as is common in one-dimensional simulations), instead of as model topography, in general would overcome this dependence on model resolution; this is an important factor to consider when deciding how to set up a flood model.

In the case study of the Bommelerwaard, the 100 m model results in the most conservative number of fatalities due to slightly larger water depths at locations with many inhabitants, such as Zaltbommel. The differences between the models regarding the number of fatalities are on the order of 7–11% compared to runs with finer model resolutions. Hence, the impact of finer model resolutions is limited for this area. This outcome is related to the exposure: the more significant differences between model outcomes were mainly found at locations with few to no inhabitants.

The differences between individual risk outcomes of the various model resolutions are more significant: the finer model resolutions have a significantly higher maximum individual risk value than the 100 m model. Since the individual risk is the dominant criterion for the safety standard in this area, this sensitivity may have

consequences for the safety standards of the dike ring. The higher resolution models resulted here in higher water level rise rates and thus in higher individual risks.

Moreover, the usage of different model resolutions results in different surface areas for the breach zone, where the assumed mortality rate is 100%. With the application of finer model resolutions, high flow velocities are found over a larger area than in the coarse resolution model. Especially when the buildings are schematised as solid objects instead of by locations with a higher hydraulic roughness, the breach zone area increases by 80% compared to the coarse resolution simulation.

This article therefore concludes that model resolution can impact the resulting flood characteristics, such as the water level rise rate and flow velocity, and therefore, influences the calculated mortality rate and individual risk outcome. For this case study, the more dangerous locations could also be identified by using the coarse model. However, in general, careful consideration of underpasses, tunnels, or culverts through blocking obstacles is required to assess the effect on the areas behind those structures.

5.2 | Sensitivity to loss of life model

The sensitivity of the mortality rate to modified factors was also tested. Three factors (water arrival time, improved building characteristics, and age) were considered and all three proved to be relevant in the case study of the Bommelerwaard.

The water arrival time was included in the approach by means of escape fractions. This study shows that the reduction of the number of people present in an area at risk by escape (in addition to evacuation) has a significant impact on the mortality rate and loss of life outcomes. The water arrival time can be long in case of flooding, especially in large dike ring areas in the Netherlands where it can be in the order of days. It is recommended to do further research on flood event management in order to estimate and increase the escape fraction since this study shows that this escape fraction may reduce the flood fatality risk considerably (by 60–65%).

This study also explored the effect of including improved building characteristics in the rapidly rising water zone and the transition zone. This modification in the loss of life estimation approach is, therefore, relevant for areas with large rise rates (> 0.5 m/hr) and sufficiently large water depths (>2.1 m). By including the improved building strength, the mortality rates in these zones were reduced, resulting in an 18% lower maximum individual risk value. However, the effect on the number of fatalities is limited, since few people are living in these areas (5% reduction). It is recommended to further investigate the relation between building quality and mortality rate (Jansen et al., 2020) to improve the mortality functions.

Finally, age was included in the approach, because the age distribution has shifted since 1953 and more elderly are present in society nowadays. By including age, an overall ($\sim$20%) increase of fatalities is expected since the elderly (>65 years) are more vulnerable to flooding. The case study of the Bommelerwaard shows that the impact on the individual risk depends on the spatial distribution of the elderly. In this study, the individual risk was not sensitive to the inclusion of age since the most dangerous neighbourhoods had a relatively young population. The relationship between age(ing) and mortality rate is recommended to be further looked into as the number of fatalities is sensitive to this.

5.3 | Overall approach

The outcomes of this study are relevant to flood risk managers and for the discussion of potential measures to reduce risks. By better models and visualisation of outcomes perhaps also other measures besides strengthening embankments to certain standards may be considered. For example, in this case study to reduce the danger in the downstream area with the high rise rate, also the old embankment (the Meidijk in Figure 1) which blocks floodwater and causes high rise rates (and which has no water retaining function anymore under daily circumstances) could be partly removed. This study may also help modellers to decide whether a more detailed model is really necessary, which as stated before, depends on the area characteristics and the aim of the modelling task. For the study described here, a higher resolution model is not needed for assessment of total number of fatalities, but it has a strong effect on the maximum individual risk values that are crucial for decision making in the Netherlands.

ACKNOWLEDGEMENTS

Funding for this project was provided by Deltares, and the Top Consortium for Knowledge and Innovation (TKI) Delta Technology Project TU02 "Building collapse and fatality during floods," which includes Deltares, TU Delft, Rijkswaterstaat, and HKV Engineers.

DATA AVAILABILITY STATEMENT

The data that support the findings of this study are available from the corresponding author upon reasonable request.

ORCID

Jeremy D. Bricker https://orcid.org/0000-0002-7503-6652

Karin M. De Bruijn https://orcid.org/0000-0003-1454-5338

REFERENCES

Aboelata, M., & Bowles, D. S. (2008). *Association of State Dam Safety Officials Annual Conference (Dam Safety 2008)*. Proceedings of a meeting held 7-11 September 2008, Indian Wells, California. Association of State Dam Safety Officials (ASDSO). (Vol. 2, p. 1434). Curran Associates, Inc. (Dec 2008).

Actueel Hoogtebestand Nederland 3 (Database for elevations in the Netherlands 3). (2019). Retrieved from https://www.ahn.nl/ahn-viewer

Apel, H., Aronica, A. G. T., Kreibich, A. H., Thieken, A. A. H., Aronica, G. T., & Thieken, A. H. (2009). Flood risk analyses-how detailed do we need to be?. *Natural Hazards* (Vol. *49*, pp. 79–98). Springer, New York.

Asselman, N. (2005). *Consequences of floods: Damage to buildings and casualties* (p. 3668). Delft, The Netherlands: WL Delft Hydraulics Report Q.

Asselman, N. (2009). Task 8: Flood inundation modelling—Model choice and proper application. T08-09-03.

Basisregistratie Adressen en Gebouwen (Database for Building Characteristics). (2017). Retrieved from https://www.kadaster.nl/bag-viewer

Bates, P. D. (2012). Integrating remote sensing data with flood inundation models: How far have we got? *Hydrological Processes*, *26* (16), 2515–2521.

Bermúdez, M., & Zischg, A. P. (2018). Sensitivity of flood loss estimates to building representation and flow depth attribution methods in micro-scale flood modelling. *Natural Hazards*, *92*(3), 1633–1648.

Beven, K. (2007). Towards integrated environmental models of everywhere: Uncertainty, data and modelling as a learning process. *Hydrology and Earth System Sciences Discussions, European Geosciences Union*, *11*(1), 460–467.

Bricker, J. D., Schwanghart, W., Adhikari, B. R., Moriguchi, S., Roeber, V., & Giri, S. (2017). Performance of models for flash flood warning and hazard assessment: The 2015 Kali Gandaki landslide dam breach in Nepal. *Mountain Research and Development*, *37*(1), 5–15.

Brussee, A. R. (2020). *Improving flood fatality risk assessment for river flooding in The Netherlands*: *Implications of alternative functions and model resolution variations on mortality and fatalities in the Bommelerwaard*. [MSc thesis]. Delft University of Technology, The Netherlands.

Chen, A. S., Hammond, M. J., Djordjevic, S., Butler, D., Khan, D. M., & Veerbeek, W. (2016). From hazard to impact: Flood damage assessment tools for mega cities. *Natural Hazards*, *82*, 857–890.

de Bruijn, K. M., & Klijn, F. (2009). Risky places in The Netherlands: A first approximation for floods. *Journal of Flood Risk Management*, *2*(1), 58–67.

de Bruijn, K. M., & Slager, K. (2014). Mortality functions in the flood impact module.

de Bruijn, K. M., & Slager, K. (2018). Leidraad voor het maken van overstromingssimulaties.

de Moel, H., van Alphen, J., & Aerts, J. C. J. H. (2009). Natural hazards and earth system sciences flood maps in Europe-methods, availability and use. *Natural Hazards and Earth System Sciences*, *9*, 289–301.

di Mauro, M., de Bruijn, K. M., & Meloni, M. (2012). Quantitative methods for estimating flood fatalities: Towards the introduction of loss of life estimation in the assessment of flood risk. *Natural Hazards*. *63*(2), 1083–1113. https://doi.org/10.1007/s11069-012-0207-4

Dottori, F., di Baldassarre, G., & Todini, E. (2013). Detailed data is welcome, but with a pinch of salt: Accuracy, precision, and uncertainty in flood inundation modeling. *Water Resources Research*, *49*(9), 6079–6085.

Ernst, J., Dewals, B. J., Detrembleur, S., Archambeau, P., Erpicum, S., Pirotton, M., … Dewals, B. J. (2010). Micro-scale flood risk analysis based on detailed 2D hydraulic modelling and high resolution geographic data. *Natural Hazards*, *55*, 181–209.

Fewtrell, T. J., Bates, P. D., Horritt, M., & Hunter, N. M. (2008). Evaluating the effect of scale in flood inundation modelling in urban environments. *Hydrological Processes*, *22*(26), 5107–5118.

Hunter, N. M., Bates, P. D., Neelz, S., Pender, G., Villanueva, I., Wright, N. G., … Mason, D. C. (2008). Benchmarking 2D hydraulic models for urban flooding. *Proceedings of the Institution of Civil Engineers - Water Management*, *161*(1), 13–30.

Jansen, L., Korswagen, P. A., Bricker, J. D., Pasterkamp, S., de Bruijn, K. M., & Jonkman, S. N. (2020). Experimental determination of pressure coefficients for flood loading of walls of Dutch terraced houses. *Engineering Structures*, *216*, 110647.

Jonkman, S. N. (2007). *Loss of life estimation in flood risk assessment*: *Theory and applications*. [PhD dissertation]. Delft University of Technology, The Netherlands.

Jonkman, S. N., Jongejan, R., & Maaskant, B. (2011). The use of individual and societal risk criteria within the Dutch flood safety policy-nationwide estimates of societal risk and policy applications. *Risk Analysis*, *31*(2), 282–300.

Jonkman, S. N., Maaskant, B., Boyd, E., & Levitan, M. L. (2009). Loss of life caused by the flooding of New Orleans after hurricane Katrina: Analysis of the relationship between flood characteristics and mortality. *Risk Analysis*, *29*(5), 676–698.

Kron, W. (2005). Flood risk = hazard • values • vulnerability. *Water International*, *30*(1), 58–68.

Landelijk Grondgebruik Nederland 6 (Database for land use in the Netherlands). (2008). Retrieved from https://www.wur.nl/nl/Onderzoek-Resultaten/Onderzoeksinstituten/Environmental-Research/Faciliteiten-Producten/Kaarten-en-GIS-bestanden/Landelijk-Grondgebruik-Nederland/Versies-bestanden/LGN6.htm

Lumbroso, D. M., Sakamoto, D., Johnstone, W. M., Tagg, A. F., & Lence, B. J. (2011). Development of a life safety model to estimate the risk posed to people by dam failures and floods. *Dams and Reservoirs*, *21*(1), 31–43.

Maaskant, B., Jonkman, S. N., & Kok, M. (2009). Analyse slachtofferaantallen VNK-2 en voorstellen voor aanpassingen slachtofferfuncties.

Mason, D. C., Horritt, M. S., Hunter, N. M., & Bates, P. D. (2007). Use of fused airborne scanning laser altimetry and digital map data for urban flood modelling. *Hydrological Processes*, *21*(11), 1436–1447.

Mignot, E., Paquier, A., & Haider, S. (2006). Modeling floods in a dense urban area using 2D shallow water equations. *Journal of Hydrology*, *327*(1–2), 186–199.

Papaioannou, G., Loukas, A., Vasiliades, L., & Aronica, G. T. (2016). Flood inundation mapping sensitivity to riverine spatial resolution and modelling approach. *Natural Hazards*, *83*(1), 117–132.

Pappenberger, F., Beven, K. J., Ratto, M., & Matgen, P. (2008). Multi-method global sensitivity analysis of flood inundation models. *Advances in Water Resources*, *31*(1), 1–14.

Parodi, M. U., Giardino, A., van Dongeren, A., Pearson, S. G., Bricker, J. D., & Reniers, A. J. H. M. (2020). Uncertainties in coastal flood risk assessments in Small Island developing states. *Natural Hazards and Earth System Sciences*, *20*(9), 2397–2414.

Priest, S. (2007). Building a model to estimate risk to life for European flood events—Middlesex University Flood Hazard Research Center, Final Report. T10-07-10. Retrieved from https://eprints.mdx.ac.uk/16266/

Projectbureau VNK2. (2011). Veiligheid Nederland in Kaart: De Methode van VNK2 nader verklaard. Retrieved from https://www.helpdeskwater.nl/onderwerpen/waterveiligheid/programma-projecten/veiligheid-nederland/publicaties/

Savage, J. T. S., Bates, P. D., Freer, J., Neal, J., & Aronica, G. (2016). When does spatial resolution become spurious in probabilistic flood inundation predictions? *Hydrological Processes*, *30*(13), 2014–2032.

Savage, J. T. S., Pianosi, F., Bates, P. D., Freer, J., & Wagener, T. (2016). Quantifying the importance of spatial resolution and other factors through global sensitivity analysis of a flood inundation model. *Water Resources Research*, *52*(11), 9146–9163.

Schubert, J. E., & Sanders, B. F. (2012). Building treatments for urban flood inundation models and implications for predictive skill and modeling efficiency. *Advances in Water Resources*, *41*, 49–64.

Shen, D., Qian, T., Chen, W., Chi, Y., & Wang, J. (2019). A quantitative flood-related building damage evaluation method using airborne LiDAR data and 2-D hydraulic model. *Water*, *11*(5), 987.

Slager, K., & Wagenaar, D. (2017). Standaardmethode 2017: Schade en slachtoffers als gevolg van overstromingen. Retrieved from https://www.helpdeskwater.nl/onderwerpen/applicaties-modellen/applicaties-per/aanleg-onderhoud/aanleg-onderhoud/schade-slachtoffer/

Slootjes, N., & van der Most, H. (2016). *Technisch-inhoudelijke uitwerking van eisen aan primaire keringen*. Retrieved from https://www.helpdeskwater.nl/onderwerpen/waterveiligheid/primaire/normen/

Slootjes, N., & Wagenaar, D. (2016). *Factsheets normering primaire waterkeringen*. Retrieved from https://www.helpdeskwater.nl/onderwerpen/waterveiligheid/primaire/normen/

Teng, J., Jakeman, A. J., Vaze, J., Croke, B. F. W., Dutta, D., & Kim, S. (2017). Flood inundation modelling: A review of methods, recent advances and uncertainty analysis. *Environmental Modelling and Software*, *90*, 201–216.

van der Sande, C. J., de Jong, S. M., & de Roo, A. P. J. (2003). A segmentation and classification approach of IKONOS-2 imagery for land cover mapping to assist flood risk and flood damage assessment. *International Journal of Applied Earth Observation and Geoinformation*, *4*(3), 217–229.

Vergrouwe, R., & Bossenbroek, J. C. (2010). Veiligheid Nederland in kaart (VNK2): Overstromingsrisico Dijkring 38 Bommelerwaard.

Yu, D., & Lane, S. N. (2006). Urban fluvial flood modelling using a two-dimensional diffusion-wave treatment, part 1: Mesh resolution effects. *Hydrological Processes*, *20*(7), 1541–1565.

How to cite this article: Brussee AR, Bricker JD, De Bruijn KM, Verhoeven GF, Winsemius HC, Jonkman SN. Impact of hydraulic model resolution and loss of life model modification on flood fatality risk estimation: Case study of the Bommelerwaard, The Netherlands. *J Flood Risk Management*. 2021; 14:e12713. https://doi.org/10.1111/jfr3.12713

APPENDIX

Inclusion of age

Jonkman (2007) compared the fractions of fatalities and the population for different age categories for the 1953 event. Based on this comparison, approximately 20% of the fatalities were assumed to be over 65 years of age while 10% of the population was over 65 years. In 2019, 19% of the population was over 65 years following the CBS. Based on these assumptions, the overall mortality rate of the event can be corrected. The Bommelerwaard has 48,110 inhabitants; hence, in 1953, 4,811 inhabitants are expected to have been over 65 years, while in 2019, this is 9,141 inhabitants. The 100 m model forms the base case of the Bommelerwaard and has 598 fatalities as a result. When 20% of the fatalities are expected to be over 65, this gives 120 fatalities, thus a mortality rate among the elderly of 2.5%. This mortality rate is used to find the expected increase in fatalities when 19% of the population is assumed 65+. This results in 229 fatalities and in a mortality rate of 1.47% for the total event.

In the second approach, age is included per neighbourhood. If the population of the neighbourhood has more than 10% people aged over 65 years (the fraction of the population 65+ in 1953), the mortality rate per grid cell within that neighbourhood is increased by 0.1% per percentage of people 65+. For example, when a neighbourhood has a percentage of 15% of the population aged over 65, the mortality rate per grid cell in that neighbourhood is increased by 0.5%. Mortality rate cannot exceed 100% and the correction is only applied if the grid cell has a mortality rate of 1% or larger. The neighbourhoods and population data of the CBS in 2008 are used.